Biosensors and Bioelectronics 24 (2009) 1437–1444

Contents lists available at ScienceDirect

Biosensors and Bioelectronics

journal homepage: www.elsevier.com/locate/bios

Electrically active polyaniline coated magnetic (EAPM) nanoparticle as novel transducer in biosensor for detection of *Bacillus anthracis* spores in food samples

Sudeshna Pal, Evangelyn C. Alocilja*

Department of Biosystems and Agricultural Engineering, Michigan State University, East Lansing, MI 48824, USA

ARTICLE INFO

Article history:
Received 14 April 2008
Received in revised form 4 August 2008
Accepted 13 August 2008
Available online 22 August 2008

Keywords:
Electrically active
Polyaniline
Direct-charge transfer
Immunomagnetic
Bacillus anthracis
Magnetic nanoparticles

ABSTRACT

Electrically active polyaniline coated magnetic (EAPM) nanoparticle-based biosensor has been developed for the detection of *Bacillus anthracis* endospores in contaminated food samples. The 100 nm-diameter EAPM nanoparticles are synthesized from aniline monomer (made electrically active by acid doping) coating the surface of gamma iron oxide cores. The magnetic, electrical, and structural characteristics of the synthesized EAPM nanoparticles have been studied using superconducting quantum interference device (SQUID), four-point probe, and transmission electron microscopy (TEM). Room temperature hysteresis of the synthesized nanoparticles shows a saturation magnetization value of 44.1 emu/g. The EAPM nanoparticles are biologically modified to act as an immunomagnetic concentrator of *B. anthracis* spores from lettuce, ground beef and whole milk samples and are directly applied to a direct-charge transfer biosensor. The detection mechanism of the biosensor depends on the capillary flow of the captured spores on the biosensor surface along with direct-charge transfer across the EAPM nanoparticles. Experimental results indicate that the biosensor is able to detect *B. anthracis* spores at concentrations as low as 4.2×10^2 spores/ml from the samples. The EAPM-based biosensor detection system is fast and reliable with a total detection time of 16 min.

1. Introduction

The use of microorganisms as biological weapons has long been reported in history. One of the first major attacks occurred in the 14th century with *Yersenia pestis* during the siege of Kaffa (Inglesby et al., 2000). The most recent was the deliberate release of *B. anthracis* spores through the postal system in the United States in October 2001, resulting in 22 cases of anthrax and 5 deaths (Jernigan et al., 2001). An optimal biological weapon is characterized by its high lethality, easy production in large quantities, environmental stability, and its capability to be readily dispersed into aerosols (i.e. 1–10 μm particle size) (Peruski and Peruski, 2003). When reviewed for these characteristics, *B. anthracis* is the most likely to be used as a biological weapon since the microorganism can form spores that can be easily aerosolized, the spore forms can survive harsh environmental conditions, and inhalational anthrax caused by *B. anthracis* has high mortality rates nearing 100% (Edwards et al., 2006). Specific identification of the microorganism involves complex and laborious microbiological methods requiring anywhere between 2 and 4 days (Inglesby, 2000). A rapid, onsite, and sensitive, detection system for *B. anthracis* has become imperative. Biosensors can serve as promising alternatives by providing early identification of such harmful pathogens. Several biosensor technologies using fluorescence resonance energy transfer (FRET), field effect transistors (FET), microcantilevers, porous silicon, quantum dots, and microimpedance have been developed for the detection of pathogens (Goldman et al., 2004; Gupta et al., 2004; Mathew and Alocilja, 2005; Patolsky et al., 2004; Radke and Alocilja, 2004). Recent trends indicate that the biosensor technology is the fastest growing technology in the field of rapid microbial pathogen detection (Lazcka et al., 2007).

Conducting polymers or polymers with a π-electron backbone have attracted considerable interest over the past two decades due to their unusual electronic properties such as, high electrical conductivity, low ionization potential, high electron affinity, and non-linear optical properties. Such polymers have found a number of practical applications in molecular electronics, electronic displays, telecommunication, electrochemical storing systems and most recently in biosensors (Hohnholz et al., 2005; Kaneto et al., 2007; Ramanavicius et al., 2006; Toyoda et al., 2005). The popularity of conducting polymers in biosensor applications can be attributed to a number of factors, such as their compatibility with biomolecules, efficient electrical charge transfer from biochemical reactions to electronic circuits, their ability to be deposited on

* Corresponding author at: Department of Biosystems and Agricultural Engineering, Michigan State University, 204 Farrall Hall, East Lansing, MI 48824, USA.
Tel.: +1 517 355 0083; fax: +1 517 432 2892.
E-mail address: alocilja@msu.edu (E.C. Alocilja).

0956-5663/$ – see front matter © 2008 Elsevier B.V. All rights reserved.
doi:10.1016/j.bios.2008.08.020

electrode surfaces, and the ability to have control over polymer layer thickness, electrical properties, and bio-reagent loading (Ahuja et al., 2007; Ryder et al., 1997). Current research interests are driven toward magnetic polymer nanostructures, a new class of materials, where magnetic nanoparticles are embedded in conducting polymer matrices. These magnetic nanostructures have immense potential for applications in electromagnetic devices, drug targeting, and electromagnetic interface shielding (Asmatulu et al., 2005; Boissiere et al., 2006; El-Tantawy et al., 2004). They have the advantages of non-corrosiveness, light weight, mechanical strength, and dielectric tunability along with novel magnetic and optical properties (Poddar et al., 2004).

Polyaniline is the most studied conducting polymer in these multi-component systems due to its unique and controllable electrical and chemical properties, excellent environmental stability, and simple and inexpensive synthetic procedures (chemical and electrochemical) (Stejskal and Gilbert, 2002). Recent literature shows that different types of magnetic cores and doping agents have been used for the synthesis of magnetic polyaniline nanoparticles (Dallas et al., 2006; Jiang et al., 2006; Li et al., 2006, 2007; Xue et al., 2006; Zhang et al., 2005). Typical examples of the magnetic cores include iron(II, III) oxide, hydroxyl iron, Ni Zn Ferrite and Li Ni Ferrite. Whereas, hydrochloric acid, β-napthalene sulfonic acid, dodecylbenzoylsulfonic acid, toluene, and phosphoric acid are commonly used doping agents in these synthetic procedures. As reported by previous authors, these magnetic polyaniline nanoparticles have sizes in the range of 30 nm and 5 μm and their magnetization values vary between 0.76 and 181 emu/g.

Literature suggests that magnetic micro- and nanoparticles have widespread application as separation tools in the purification of nucleic acids, proteins and peptides, bacteria, and metals, such as copper, because of their ability to quickly agglomerate and resuspend in response to changes in magnetic forces (Liang et al., 2007; Park and Chang, 2007). In this study, we have exploited the electrical and magnetic properties of electrically active polyaniline coated magnetic (EAPM) nanoparticles to use them as a novel tool for magnetic concentration of targets and signal transduction in biosensors. These EAPM nanoparticles in biosensors can provide several advantages, such as increased surface to volume ratio for biological events owing to their nanoscale dimensions, increased assay kinetics due to close proximity to targets, magnetic manipulation of the nanoparticles, and minimized matrix interference from complex samples (such as food and clinical specimens). In this paper, we describe an EAPM nanoparticle-based direct-charge transfer biosensor for concentration and detection of *B. anthracis* spores from complex food matrices. We present characterization studies for the synthesized EAPM nanoparticles, the biosensor performance of the nanoparticles in lettuce, whole milk, and ground beef samples, and the specificity of the biosensor in non-target pathogens. The efficiency of the EAPM nanoparticles in magnetic concentration of *B. anthracis* spores from the food samples is also included in the paper.

2. Materials and methods

2.1. Biosensor design and detection scheme

In this experimental study, the biosensor design was adapted and modified from a direct-charge transfer biosensor previously developed by the authors (Pal et al., 2007). In the modified design (Fig. 1a), the biosensor consists of three disposable membrane pads: sample application pad, capture pad, and absorption pad. The overall biosensor dimension along with the dimensions of each membrane pad has also been tabulated in Fig. 1a. Silver electrodes were fabricated along both sides on the capture pad leaving an electrode gap of 0.5 mm. For data acquisition, the biosensor units were connected to a handheld multimeter linked with a computer.

Fig. 1b is a schematic representation of the immunomagnetic separation and biosensor detection procedure. The biosensor detection involves a sandwich immunoassay, with a capture antibody (IgG) immobilized on the biosensor capture pad and a detector antibody (IgG) conjugated with synthesized EAPM nanoparticles. The detector antibody conjugated EAPM nanoparticles are added to the *B. anthracis* spore contaminated food samples (Fig. 1b, step 1) and used to immunomagnetically concentrate the spores from the complex food matrices (step 2). The concentrated targets are then washed to remove unbound materials (step 3) and applied to the sample application pad of the biosensor (step 4). The antigen-antibody–EAPM complex flows to the capture pad, where the antigen is anchored by the capture antibodies present and a sandwich complex is formed (step 5). The conductive EAPM nanoparticles bound to the antigens in the sandwich act as a voltage controlled "ON" switch resulting in decreased resistance across the silver electrodes which is recorded electrically (step 6) (Pal et al., 2007, 2008).

2.2. Chemicals and reagents

Aniline, iron(III) oxide nanopowder, glutaraldehyde, polysorbate 20 (Tween 20), hydrochloric acid (1N), ammonium peroxy disulfate, tris buffer, peptone water, and sodium phosphate (dibasic and monobasic) were purchased from Sigma–Aldrich (St. Louis, MO). Mouse monoclonal anti-anthrax IgG (clone 2C3) and polyclonal goat anti-anthrax combo IgG molecules were obtained from Chemicon International (Millipore, CA) whereas anti-goat IgG-FITC (whole molecule) was obtained from Sigma–Aldrich (St. Louis, MO). Nitrocellulose and cellulose acetate membrane pads for the biosensor were purchased from Millipore (Bedford, MA). Conductive micro-tip pen used for dispensing silver electrodes were procured from Chemtronics (Kennesaw, GA). De-ionized water from Millipore Direct-Q system was used for preparing all reagents.

2.3. Bacterial isolates and spores

Characterized strains of *B. anthracis* (Sterne) were obtained from the Michigan Department of Community Health (Lansing, MI). Generic *Escherichia coli* and *Salmonella enterica* serovar Enteritidis (S-64) strains were procured from the collection of the Biosensors Laboratory at Michigan State University. The *B. anthracis* and *E. coli* strains were grown in trypticase soy broth (BD Biosciences, MD), while lactose broth (BD Biosciences, MD) was used for growing *S.* Enteritidis cultures. The cultures were grown at 37 °C for 24 h.

Sporulation of *B. anthracis* Sterne strain was promoted following a previously published protocol (Pezard et al., 1991). The spore count was estimated using a cell counting chamber (Hemocytometer) and viable spores were enumerated by microbial plating in trypticase soy agar(II) with 5% sheep blood plates (BD Biosciences, MD). The plating and colony counting experiments were performed using automated spiral plater and colony counter equipments (Microbiology International, MD).

2.4. EAPM nanoparticle synthesis and characterization studies

The EAPM nanoparticles were synthesized from aniline monomer (made electrically active by acid doping) and gamma-iron(III) oxide (γ-Fe_2O_3) nanoparticles using a chemical synthesis procedure (Sharma et al., 2005). The γ-Fe_2O_3 to monomer weight ratio was maintained at 1:0.6 in the synthesis procedure.

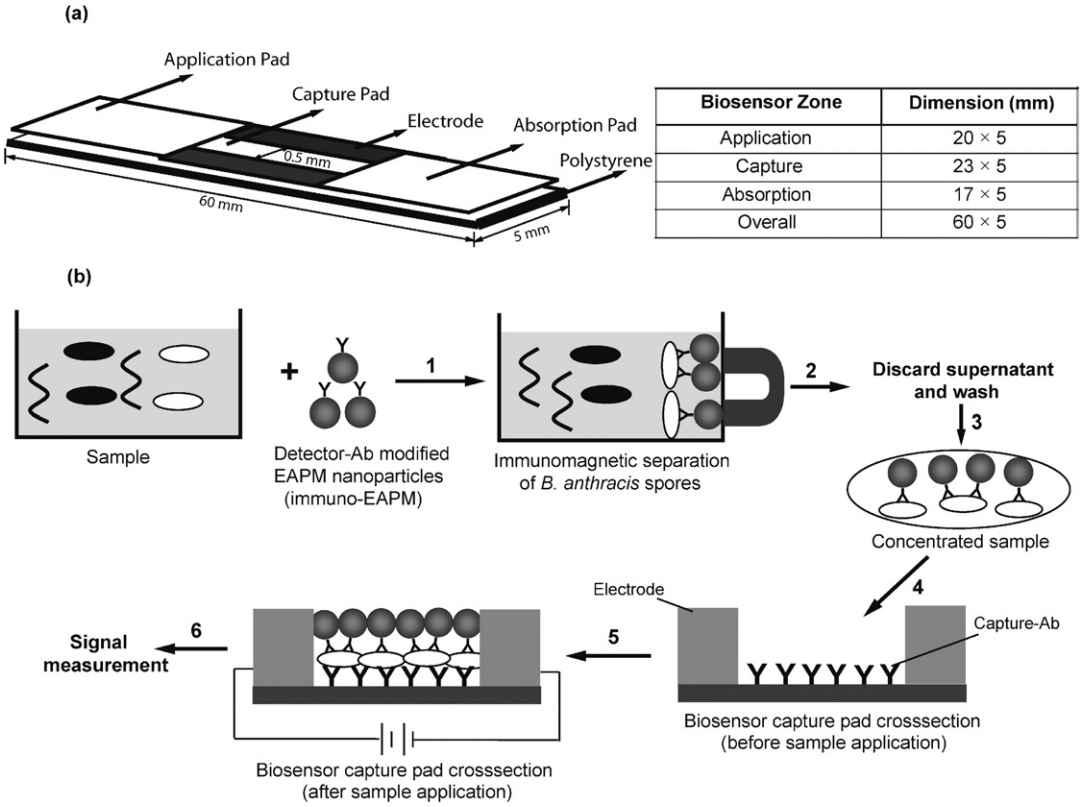

Biosensor Zone	Dimension (mm)
Application	20 × 5
Capture	23 × 5
Absorption	17 × 5
Overall	60 × 5

Fig. 1. (a) Biosensor architecture and dimensions and (b) schematic representation of the biosensor detection system.

A superconducting quantum interference device (Quantum Design MPMS SQUID) magnetometer was used for magnetic characterization studies of the synthesized EAPM nanoparticles. For hysteresis loop measurement, the nanoparticles were subjected to a magnetic field cycling between +15 and −15 kOe, while the temperature was maintained constant at 300 K. Electrical conductivity of the synthesized EAPM nanoparticles was evaluated in solid form. The nanoparticles were compressed into pellets and electrical conductivity was measured at room temperature using a Four Point Probe (Lucas/Signaton Corporation, Pro4; CA). The structural morphology and size distribution of the nanoparticles were studied using a 200 kV field emission transmission electron microscope (JEOL 2200 FS).

2.5. Bio-modification of EAPM nanoparticles

The synthesized EAPM nanoparticles were conjugated with mouse monoclonal anti-*B. anthracis* IgG molecules by direct physical adsorption of the antibodies on the nanoparticles. Anti-*B. anthracis* IgG (150 μg/ml) was mixed with the EAPM nanoparticles (100 mg/ml) in 100 mM phosphate buffer (pH 7.4). The reaction mixture was incubated for 1 h at 25 °C in a rotational hybridization oven (Amerex Instruments, Inc. CA). After incubation, the IgG modified nanoparticles (immuno-EAPMs) were magnetically separated to remove the supernatant using a magnetic separator (Spherotech, IL). The immuno-EAPMs were washed three times with a blocking buffer consisting of 100 mM Tris–HCl buffer (pH 7.6) and 0.1% (w/v) casein. Finally, the immuno-EAPMs were suspended in 100 mM phosphate buffer (pH 7.4) and stored at 4 °C. The bio-modification of the EAPM nanoparticles was investigated by measuring the absorption of IgG molecules before and after reaction with the nanoparticles using a UV–vis–NIR scanning spectrophotometer (UV-3101PC, Shimadzu, Kyoto, Japan).

2.6. Fabrication of the biosensor

The nitrocellulose biosensor capture membrane pads were first cleaned with de-ionized water followed by 10% methanol (v/v) for 45 min and dried at room temperature. The cleaned membranes were treated with 0.5% glutaraldehyde solution (v/v) for 1 h. The glutaraldehyde activated capture membranes were coated with polyclonal goat anti-*B. anthracis* IgG (500 μg/ml) using a reagent dispensing module (Matrix 1600, Kinematic Automation Inc., CA) and the antibody treated membranes were then incubated for 1 h at 37 °C. Finally, the membrane surface was washed with blocking buffer consisting of 100 mM Tris–HCl buffer (pH 7.6) and 0.1% (v/v) Tween 20 and incubated for 45 min at 37 °C. The antibody modified membranes were dried at room temperature and stored at 4 °C. The anti-*B. anthracis* IgG attachment on the capture pad was confirmed by secondary FITC anti-goat IgG molecules as label using a laser scanning confocal microscope (Olympus Fluoview 1000). The application and the absorption cellulose membrane pads were washed with de-ionized water to remove dirt and surface residues and dried at room temperature.

2.7. Food sample preparation

Romaine lettuce, lean ground beef, and ultra-pasteurized whole milk, was purchased from a local grocery store. For the lettuce and beef samples, 25-g samples were weighed, mixed with 225 ml of 0.1% (w/v) peptone water in a Whirl-Pak plastic bag, and stomached in a stomacher (Microbiology International, MD) for 1 min. The whole milk samples were used as purchased. Nine milliliters of the three kinds of liquid samples were thoroughly mixed with 1 ml of appropriate concentrations of *B. anthracis* spore stock solution in a Vortex mixer (Fisher Scientific, IA). Finally, a series of 10 ml sam-

ples inoculated with *B. anthracis* spores at concentrations ranging from 10^1 to 10^7 spores/ml were obtained.

2.8. Target capture and biosensor detection

The immuno-EAPMs were added to different concentrations of the *B. anthracis* spore inoculated food samples (4.2×10^1 to 4.2×10^7 spores/ml) in order to have a final immuno-EAPM concentration of 20 mg/ml. This was followed by 10-min incubation with gentle shaking at room temperature. The immuno-EAPM-spore complexes formed were magnetically separated from the unbound spores and food matrices, to remove the supernatant, and washed twice with sterile de-ionized water before re-suspending in 10 ml 0.1% (w/v) peptone water. A control or blank solution containing the same concentration of the immuno-EAPMs but with no *B. anthracis* spores in 0.1% (w/v) peptone water was simultaneously prepared for each food sample.

For the detection process, the biosensor units were connected to a hand-held multimeter (BK Precision, AK-2880A, MA) with RS-232 interface and linked to a computer. One hundred microliters of the captured immuno-EAPM-spore complexes was applied to the application pad on the biosensor and the resistance signal across the silver electrodes was recorded. Resistance measurements were made both before and after sample application. The flow time of the sample from application membrane to capture membrane was approximately 1 min and data recording for each sample was carried through 6 min. For each experiment, a minimum of three replications were performed. The biosensors were calibrated against corresponding control solutions. All biosensor experiments were performed in a Biosafety Level II Laboratory.

2.9. Biosensor specificity study

Pure spore suspensions of *B. anthracis*, and pure cultures of generic *E. coli* and *S.* Enteritidis were used for evaluating specificity of the EAPM biosensor. The immuno-EAPMs were added to 10 ml solutions of the appropriate concentration of the desired bacteria to a final immuno-EAPM concentration of 20 mg/ml. The immunomagnetic concentration and biosensor detection procedure was similar to that as described in Section 2.8. Generic *E. coli* cell concentrations ranging from 1.7×10^1 to 1.7×10^5 CFU/ml in sterile 0.1% (w/v) peptone water, *S.* Enteritidis cell concentrations ranging from 1.6×10^1 to 1.6×10^5 CFU/ml in sterile 0.1% (w/v) peptone water, and *B. anthracis* spore concentrations ranging from 4.2×10^1 to 4.2×10^5 in sterile water were used for specificity studies. The control solutions consisted of EAPM nanoparticles suspended in 0.1% (w/v) peptone water or sterile water to a final concentration of 20 mg/ml.

3. Results and discussion

Fig. 2a shows the magnetization versus magnetic field, i.e. the *M–H* loop measurements of both unmodified Fe_2O_3 and synthesized EAPM nanoparticles, using a DC SQUID magnetometer at 300 K. Both systems showed tendency to saturate at 15 kOe. The saturation magnetization (M_S) for the Fe_2O_3 nanoparticles was found to be 64.4 emu/g, whereas for the EAPM nanoparticles, the saturation magnetization reached 44.1 emu/g. The decrease in M_S value for the EAPM nanoparticles is expected due to surface interactions between the polymer (polyaniline), which is diamagnetic in nature, and iron oxide nanoparticles (Alam et al., 2007). The remanent magnetization M_r for the Fe_2O_3 and the EAPM nanoparticles were found to be 14.2 and 10.4 emu/g, respectively, and the coercive force H_c for both nanoparticles were 200 Oe. The low values of M_r and H_c suggest that the nanoparticles are still in the ferromagnetic phase

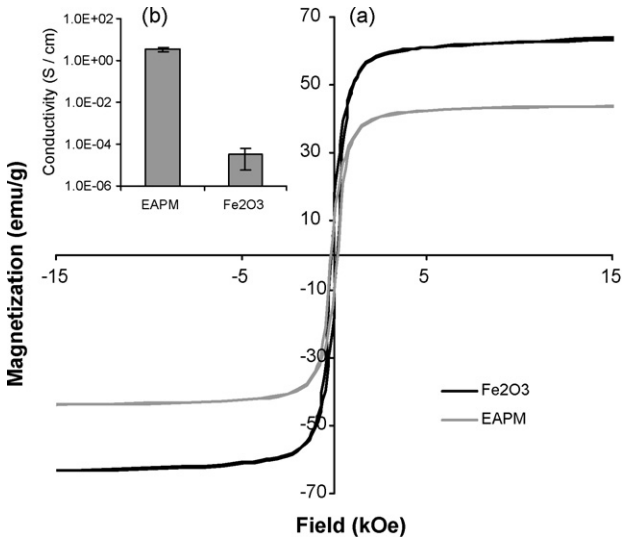

Fig. 2. (a) Experimental *M–H* curves of the synthesized EAPM and unmodified Fe_2O_3 nanoparticles at 300 K and (b) electrical conductivity measurements for the EAPM and Fe_2O_3 nanoparticles at room temperature.

but approached superparamagnetic behaviour (Kryszewski and Jeszka, 1998). Fig. 2b shows electrical conductivity measurements of both synthesized EAPM and unmodified Fe_2O_3 nanoparticles compressed into pellets of 2000-μm thickness at room temperature. The Fe_2O_3 nanoparticles have an electrical conductivity as low as 3.4×10^{-5} S/cm whereas, conductivity of the EAPM nanoparticles increases by five orders of magnitude to 3.3 S/cm. This increase in electrical conductivity is expected and confirms the presence of electrically active polyaniline in the nanoparticles.

Fig. 3a and b reveal transmission electron microscope (TEM) images of the unmodified Fe_2O_3 nanoparticles and the polyaniline coated EAPM nanoparticles. The iron oxide nanoparticles have an average diameter of 20 nm according to manufacturer's specifications which is found to be consistent with the TEM image in Fig. 3a, whereas the polyaniline coated EAPM nanoparticles shows diameter ranging from 50 to 100 nm (Fig. 3b).

Physical adsorption has been used for bio-modification of the EAPM nanoparticles with IgG molecules because the conjugation procedure is simple and allows IgG molecules to retain their activity and conformation (Zhou et al., 2004). The UV spectrum of pure anti-*B. anthracis* IgG (150 μg/ml) molecules and the unreacted IgG molecules in the supernatant after magnetic separation of immuno-EAPMs was measured by a UV–vis–NIR scanning spectrophotometer (Supplemental Information, Fig. S1). Literature suggests that IgG adsorption occurs preferentially through Fc fragment of the molecule (Buijs et al., 1996). Hence, electrostatic interactions between negatively charged Fc fragment of IgG molecules and positively charged polymer surfaces in the EAPM nanoparticles might play a significant role in the adsorption process. The immobilization of polyclonal goat anti-*B. anthracis* IgG on the biosensor capture pad was detected by secondary FITC anti-goat IgG and confirmed by fluorescent images obtained from a laser scanning confocal microscope (Supplemental Information, Fig. S2).

Fig. 4a–c show the average resistance readings measured with the EAPM nanoparticle-based direct-charge transfer biosensor in lettuce, whole milk, and ground beef samples inoculated with *B. anthracis* spores. The average resistance signals obtained from three replicates were plotted for the control and the food samples, contaminated with spore concentrations ranging from 4.2×10^1 to 4.2×10^7 spores/ml. As observed, the resistance values recorded

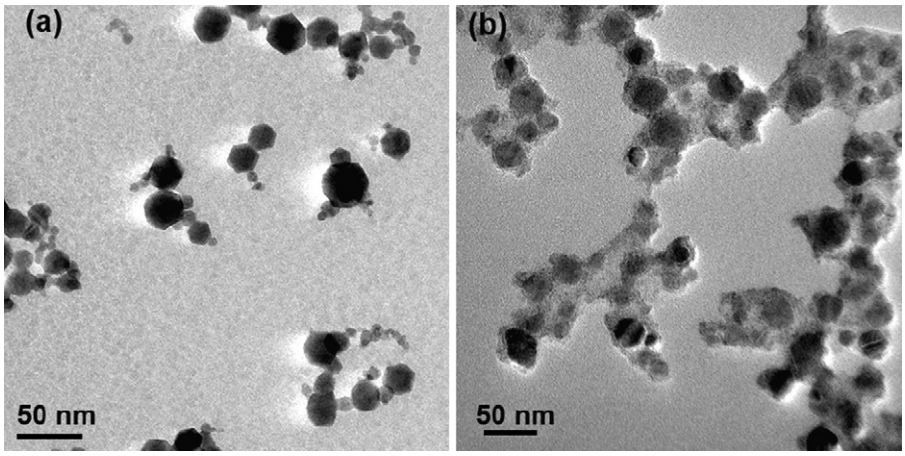

Fig. 3. TEM images of (a) unmodified Fe_2O_3 nanoparticles and (b) synthesized EAPM nanoparticles.

for the different spore concentrations are much lower than the values for the control solution that has no spores in it. The average resistances for the control solutions for all three food samples are in the range of 288 ± 50 and 353 ± 51 kΩ, whereas the average resistances for the different spore concentrations in the three food samples vary from 75.1 ± 14 to 132.6 ± 19 kΩ. The reduced resistance values support the formation of a sandwich complex on the capture pad (Fig. 1b), where the conductive EAPM nanoparticles act as a charge transfer agent causing a drop in the resistance signal across the silver electrodes (Kim et al., 2000; Pal et al., 2007). Single factor analysis of variance (ANOVA) to a significance of 95% ($P < 0.05$) was used to compare the differences in the resistance values between the control and the different spore concentrations. The lowest spore concentration that produced a resistance signal significantly different ($P < 0.05$) from the control was considered to be the sensitivity or detection limit of the biosensor. For the lettuce and ground beef samples, the biosensor sensitivity was determined to be 4.2×10^2 spores/ml with statistically significant differences from the control (P-value for lettuce at 10^2 spores/ml was 1.79E−05; P-value for ground beef at 10^2 spores/ml was

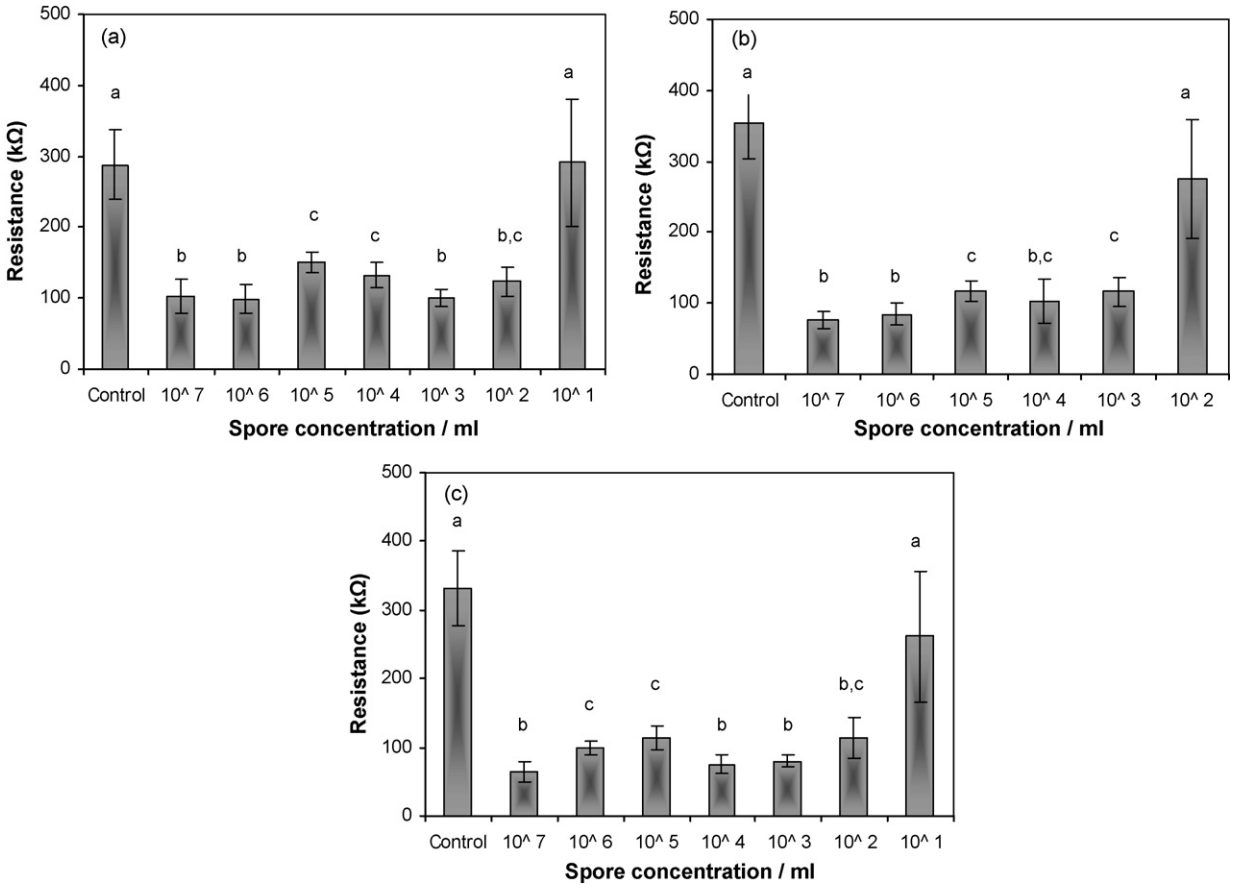

Fig. 4. The EAPM nanoparticle-based direct-charge transfer biosensor resistance responses in (a) romaine lettuce, (b) whole milk and (c) ground beef samples contaminated with *Bacillus anthracis* spores. Average resistances with the same letters are not significantly different ($P > 0.05$).

2.63E−06). For whole milk samples, the biosensor could reach a sensitivity of 4.2×10^3 spores/ml where statistically significant differences could be observed from the control (*P*-value at 10^3 spores/ml was 8.47E-08). The reduced biosensor sensitivity in the whole milk samples could be attributed to the high fat content in these samples. As observed in Fig. 4, although the biosensor resistance readings recorded for the different spore concentrations were different from the control, statistical analysis did not reveal any significant differences between the concentrations. Artifacts in biosensor fabrication, probabilistic antigen–antibody interactions, antibody orientations, and stability of the sandwich complex on the capture pad might be some of the factors behind such biosensor performance. At this stage the biosensor is only considered to be as a qualitative device for a yes/no diagnosis of *B. anthracis* spores. However, the biosensor shows excellent sensitivity and fast detection time in comparison to the very few rapid detection systems for *B. anthracis* in food matrices that have been reported in the literature (Tims and Lim, 2004; Cheun et al., 2001).

Fig. 5 shows the specificity analysis of the EAPM nanoparticle-based direct-charge transfer biosensor. A comparison of the biosensor resistance responses in pure cultures of *E. coli* with cell concentrations ranging from 1.7×10^1 to 1.7×10^5 CFU/ml, in pure cultures of *S.* Enteritidis with cell concentrations ranging from 1.6×10^1 to 1.6×10^5 CFU/ml, and pure spore suspensions of *B. anthracis* with spore concentrations ranging from 4.2×10^1 to 4.2×10^5 spores/ml, is presented in this figure. As evident in Fig. 5, the biosensor average resistance values for different concentrations of the non-target bacteria (i.e. *E. coli* and *S.* Enteritidis) are similar to the values observed for the control. Single factor analysis of variance tests to a significance of 95% ($P < 0.05$) showed no statistically significant differences between the control and different cell concentrations of *E. coli* and *S.* Enteritidis with *P*-values ranging from 0.278 to 0.887 for *E. coli*, and from 0.348 to 0.981 for *S.* Enteritidis. The results indicate that the effects of non-specific interactions are not significant for the range of cell concentrations tested on the biosensor. In comparison, for pure *B. anthracis* spore suspensions (Fig. 5), the biosensor average resistance responses show significant differences between the control and spore concentrations ranging from 10^2 to 10^5 spore/ml (*P*-value range: 0.009–0.0009) which is expected since the antibodies used in the biosensor are specific for *B. anthracis*. However, at a low *B. anthracis* spore concentration of 10^1 spores/ml, the biosensor resistance response is similar to that of the control which implies no detection at this concentration (*P*-value: 0.7).

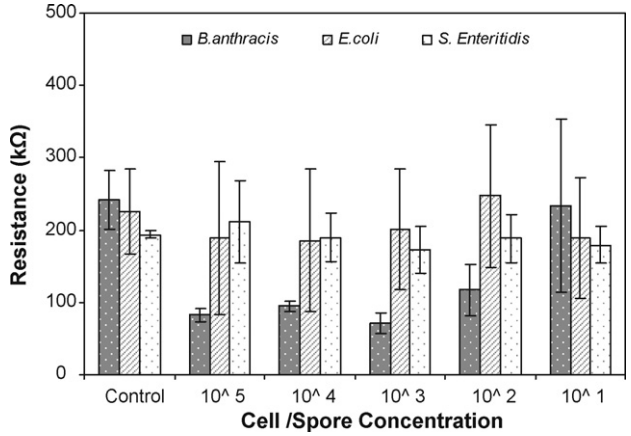

Fig. 5. Comparison of the EAPM nanoparticle-based direct-charge transfer biosensor resistance response between pure spore suspensions of *B. anthracis* and pure cultures of generic *Escherichia coli* and *S.* Enteritidis.

Table 1
Capture efficiency of the immuno-EAPM conjugates in romaine lettuce, whole milk, and ground beef contaminated with *Bacillus anthracis* spores

Dilution factor	Actual viable spore count, C_{actual} (CFU/ml)	Romaine lettuce		Whole milk		Ground beef	
		No. of captured viable spores ± S.D. ($n = 3$), $C_{captured}$ (CFU/ml)	Capture ratio (CR)	No. of captured viable spores ± SD ($n = 3$), $C_{captured}$ (CFU/ml)	Capture ratio (CR)	No. of captured viable spores ± SD ($n = 3$), $C_{captured}$ (CFU/ml)	Capture ratio (CR)
10^1	1.52×10^7	$6.07 \times 10^6 \pm 55.3$	0.40	$1.41 \times 10^6 \pm 10.5$	0.09	$3.02 \times 10^6 \pm 32.5$	0.20
10^2	1.52×10^{6a}	$2.30 \times 10^5 \pm 15.8$	0.15	$1.63 \times 10^5 \pm 10.3$	0.11	$3.17 \times 10^5 \pm 34.4$	0.21
10^3	1.52×10^{5a}	$3.40 \times 10^4 \pm 17.6$	0.22	$1.22 \times 10^4 \pm 8.2$	0.08	$2.85 \times 10^4 \pm 6.5$	0.19
10^4	1.52×10^{4a}	$2.23 \times 10^3 \pm 11.5$	0.15	$9.10 \times 10^2 \pm 19.5$	0.06	$1.38 \times 10^3 \pm 14.8$	0.09
10^5	1.52×10^{3a}	$5.53 \times 10^2 \pm 7.1$	0.36	$1.40 \times 10^2 \pm 2.6$	0.09	$5.10 \times 10^2 \pm 9.5$	0.34
10^6	1.52×10^{2a}	$1.47 \times 10^2 \pm 1.1$	0.97	$1.00 \times 10^1 \pm 0.5$	0.07	$1.10 \times 10^2 \pm 0.6$	0.72
10^7	1.52×10^{1a}	$1.00 \times 10^1 \pm 1.1$	0.66	0	0.00	$1.00 \times 10^1 \pm 1.2$	0.66
10^8	1.52×10^{0a}	0	0	0	0	0	0
Control	0	0	0	0	0	0	0

S.D. = standard deviation and n = no. of replicates.
[a] Estimated spore concentrations.

The immunomagnetic capture of *B. anthracis* spores using EAPM nanoparticles from the three different food matrices was confirmed by microbial plating in TSA II blood agar plates and the capture efficacy of the nanoparticles was evaluated. Results of the microbial plating data have been elaborated in Table 1. One hundred microliters of the captured immuno-EAPM-spore complexes were used for microbial plating and the viable spore count was enumerated after 16–36 h. The capture ratio (CR) of the EAPM nanoparticles was evaluated using the formula $CR = C_{captured}/C_{actual}$, where, C_{actual} is the actual concentration of viable spores in the sample, and $C_{captured}$ is the concentration of viable spores extracted from the food samples. As seen in Table 1, the capture effects of the EAPM nanoparticles on *B. anthracis* spores from the lettuce and ground beef samples are quite similar. In both samples, the capture effect is highest at a viable spore concentration of 1.52×10^2 CFU/ml with a CR value of 0.97 for lettuce and that of 0.72 for ground beef. Also, the EAPM nanoparticles could achieve an immunomagnetic capture at viable spore concentration as low as 1.52×10^1 CFU/ml from both lettuce and ground beef samples. However, for whole milk samples, the immunomagnetic capture of the viable *B. anthracis* spores could only go as low as 1.52×10^2 CFU/ml and the capture effects are observed to be similar for all viable spore concentrations with CR values in the range of 0.06 and 0.11. This could be explained by the high fat content of the whole milk samples which might have interfered in the immunomagnetic capture process. The capture efficiency of the EAPM nanoparticles as observed from Table 1 is found to be better than that of commercially available immunomagnetic beads which can capture only as low as 10^4 CFU/ml (Madonna et al., 2003).

4. Conclusion

This study describes a novel integrated design of using electrically active polyaniline coated magnetic nanoparticles as a magnetic concentrator and biosensor transducer in one system. The biosensor detection system is fast and includes a magnetic concentration time of 10 min followed by a signal detection time of 6 min. The sensitivity of the biosensor in the detection of *B. anthracis* spores from complex food matrices was found to be 4.2×10^2 spores/ml in lettuce and ground beef, and 4.2×10^3 spores/ml in whole milk. The EAPM nanoparticles also showed excellent capture efficiency from the food samples with a highest capture ratio of 0.97. Our results indicate that the EAPM nanoparticles have great potential in biosensing applications. Future research work will involve in advancing the electrical and magnetic properties of the nanoparticles for biosensor detection of diverse targets. Furthermore, the easy-to-use EAPM biosensor described in this study has the potential to be applied as a rapid detection device in biodefense and diagnostics.

Acknowledgements

This publication was developed under DHS Science and Technology Assistance Agreement No. 2007-ST-061-000003 awarded by the U.S. Department of Homeland Security. It has not been formally reviewed by DHS. The views and conclusions contained in this document are those of the authors and should not be interpreted as necessarily representing the official policies, either expressed or implied, of the U.S. Department of Homeland Security. The Department of Homeland Security does not endorse any products or commercial services mentioned in this publication. The authors would like to thank Dr. F.P. Downes of the Michigan Department of Community Health, Lansing, Michigan, for suggestions in microbiological procedures, and Ms. Hanna Miller, a professorial assistant (PA) of the PA training through the National Science Foundation grant number BES0508320, for assistance in research work.

Appendix A. Supplementary data

Supplementary data associated with this article can be found, in the online version, at doi:10.1016/j.bios.2008.08.020.

References

Ahuja, T., Mir, I.A., Kumar, D., Rajesh, 2007. Biomaterials 28 (5), 791–805.
Alam, J., Riaz, U., Ahmad, S., 2007. Journal of Magnetism and Magnetic Materials 314 (2), 93–99.
Asmatulu, R., Zalich, M.A., Claus, R., Riffle, J.S., 2005. Journal of Magnetism and Magnetic Materials 292, 108–119.
Boissiere, M., Meadows, P.J., Brayner, R., Helary, C., Livage, J., Coradin, T., 2006. Journal of Materials Chemistry 16 (12), 1178–1182.
Buijs, J., vandenBerg, P.A.W., Lichtenbelt, J.W.T., Norde, W., Lyklema, J., 1996. Journal of Colloid and Interface Science 178 (2), 594–605.
Cheun, H.I., Makino, S.I., Watarai, M., Shirahata, T., Uchida, I., Takeshi, K., 2001. Journal of Applied Microbiology 91 (3), 421–426.
Dallas, P., Moutis, N., Devlin, E., Niarchos, D., Petridis, D., 2006. Nanotechnology 17 (19), 5019–5026.
Edwards, K.A., Clancy, H.A., Baeumner, A.J., 2006. Analytical and Bioanalytical Chemistry 384 (1), 73–84.
El-Tantawy, F., bdel-Kader, K.M., Kaneko, F., Sung, Y.K., 2004. European Polymer Journal 40 (2), 415–430.
Goldman, E.R., Clapp, A.R., Anderson, G.P., Uyeda, H.T., Mauro, J.M., Medintz, I.L., Mattoussi, H., 2004. Analytical Chemistry 76 (3), 684–688.
Gupta, A., Akin, D., Bashir, R., 2004. Applied Physics Letters 84 (11), 1976–1978.
Hohnholz, D., Okuzaki, H., Macdiarmid, A.G., 2005. Advanced Functional Materials 15 (1), 51–56.
Inglesby, T.V., 2000. JAMA-Journal of the American Medical Association 283 (15), 1963.
Inglesby, T.V., Dennis, D.T., Henderson, D.A., Bartlett, J.G., Ascher, M.S., Eitzen, E., Fine, A.D., Friedlander, A.M., Hauer, J., Koerner, J.F., Layton, M., McDade, J., Osterholm, M.T., O'Toole, T., Parker, G., Perl, T.M., Russell, P.K., Schoch-Spana, M., Tonat, K., 2000. JAMA-Journal of the American Medical Association 283 (17), 2281–2290.
Jernigan, J.A., Stephens, D.S., Ashford, D.A., Omenaca, C., Topiel, M.S., Galbraith, M., Tapper, M., Fisk, T.L., Zaki, S., Popovic, T., Meyer, R.F., Quinn, C.P., Harper, S.A., Fridkin, S.K., Sejvar, J.J., Shepard, C.W., McConnell, M., Guarner, J., Shieh, W.J., Malecki, J.M., Gerberding, J.L., Hughes, J.M., Perkins, B.A., 2001. Emerging Infectious Diseases 7 (6), 933–944.
Jiang, J., Li, L.C., Xu, F., 2006. Chinese Journal of Chemistry 24 (12), 1804–1809.
Kaneto, K., Fujisue, H., Kunifusa, M., Takashima, W., 2007. Smart Materials & Structures 16 (2), S250–S255.
Kim, J.H., Cho, J.H., Cha, G.S., Lee, C.W., Kim, H.B., Paek, S.H., 2000. Biosensors & Bioelectronics 14 (12), 907–915.
Kryszewski, M., Jeszka, J.K., 1998. Synthetic Metals 94 (1), 99–104.
Lazcka, O., Del Campo, F.J., Munoz, F.X., 2007. Biosensors & Bioelectronics 22 (7), 1205–1217.
Li, G., Yan, S., Zhou, E., Chen, Y., 2006. Colloids and Surfaces A: Physicochemical and Engineering Aspects 276 (1–3), 40–44.
Li, X., Shen, J.Y., Wan, M.X., Chen, Z.J., Wei, Y., 2007. Synthetic Metals 157 (13–15), 575–579.
Liang, Y.Y., Zhang, L.M., Li, W., Chen, R.F., 2007. Colloid and Polymer Science 285 (11), 1193–1199.
Madonna, A.J., Van Cuyk, S., Voorhees, K.J., 2003. Rapid Communications in Mass Spectrometry 17 (3), 257–263.
Mathew, F.P., Alocilja, E.C., 2005. Biosensors & Bioelectronics 20 (8), 1656–1661.
Pal, S., Alocilja, E.C., Downes, F.P., 2007. Biosensors & Bioelectronics 22 (9/10), 2329–2336.
Pal, S., Setterington, E.B., Alocilja, E.C., 2008. IEEE Sensors Journal 8 (6), 647–654.
Park, M.E., Chang, J.H., 2007. Materials Science & Engineering C: Biomimetic and Supramolecular Systems 27 (5–8), 1232–1235.
Patolsky, F., Zheng, G.F., Hayden, O., Lakadamyali, M., Zhuang, X.W., Lieber, C.M., 2004. Proceedings of the National Academy of Sciences of the United States of America 101 (39), 14017–14022.
Peruski, A.H., Peruski, L.F., 2003. Clinical and Diagnostic Laboratory Immunology 10 (4), 506–513.
Pezard, C., Berche, P., Mock, M., 1991. Infection and Immunity 59 (10), 3472–3477.
Poddar, P., Wilson, J.L., Srikanth, H., Morrison, S.A., Carpenter, E.E., 2004. Nanotechnology 15 (10), S570–S574.
Radke, S.M., Alocilja, E.C., 2004. IEEE Sensors Journal 4 (4), 434–440.
Ramanavicius, A., Ramanaviciene, A., Malinauskas, A., 2006. Electrochimica Acta 51 (27), 6025–6037.
Ryder, K.S., Morris, D.G., Cooper, J.M., 1997. Biosensors & Bioelectronics 12 (8), 721–727.

Sharma, R., Lamba, S., Annapoorni, S., Sharma, P., Inoue, A., 2005. Journal of Applied Physics 97 (1).
Stejskal, J., Gilbert, R.G., 2002. Pure and Applied Chemistry 74 (5), 857–867.
Tims, T.B., Lim, D.V., 2004. Journal of Microbiological Methods 59 (1), 127–130.
Toyoda, E., Matsumoto, M., Handa, T., Miyata, Y., Miyajima, Y., Ichino, T., 2005. IEEE Transactions on Dielectrics and Electrical Insulation 12 (1), 175–182.
Xue, W.Y., Qiu, H., Fang, K., Li, J., Zhao, J.W., Li, M., 2006. Synthetic Metals 156 (11–13), 833–837.
Zhang, Z.M., Wan, M.X., Wei, Y., 2005. Nanotechnology 16 (12), 2827–2832.
Zhou, J., Tsao, H.K., Sheng, Y.J., Jiang, S.Y., 2004. Journal of Chemical Physics 121 (2), 1050–1057.